Lasers in Manufacturing Conference 2021

Fundamental characteristics of fiber laser beam sawing of 10 mm thick stainless steel

Madlen Borkmann[a*], Achim Mahrle[a], Patrick Herwig[a], Andreas Wetzig[a]

[a]*Fraunhofer-Institut für Werkstoff- und Strahltechnik IWS, Winterbergstraße 28, 01277 Dresden, Germany*

Abstract

AISI 304 stainless steel plates of 10 mm thickness were sectioned by fibre laser beam sawing trials. The applied sawing technique as a new variant of laser cutting with an oscillating beam relies on periodical changes of the focusing length of the optical setup by integrated mirrors with adjustable curvature radius. As a result, the focal plane position can be forced to oscillate with a frequency of up to 4800 Hz and amplitudes up to 6 mm. The resulting temporally averaged beam profile is characterized by a nearly constant beam diameter over the whole spatial oscillation range. Variations of oscillation frequency, amplitude and nominal focal layer position were performed to get first insights into the effect mechanisms of fibre laser beam sawing. It is found that the cut kerf geometry can be adjusted to improve cutting gas flow characteristics and melt removal.

Keywords: laser beam sawing; laser beam oscillation; fiber laser fusion cutting; cut kerf geometry; cutting gas flow; gas flow simulation

1. Introduction

Laser beam fusion cutting is an established process for cutting a variety of materials. A high-intensity laser beam and a high-pressure inert gas jet act together, mostly in a coaxial configuration. The laser beam is partly absorbed by the surface and melts the material whereas the gas jet transfers momentum to the melt and removes it from the developing cut kerf (Steen, 1998). The cutting process is assessed based on the achievable cutting speed, the process stability, the cut edge roughness and squareness and the dross attachments at the bottom corner.

* Corresponding author. Tel.: +49 351 83391 3720; fax: +49 83391 3300.
E-mail address: madlen.borkmann@iws.fraunhofer.de.

Various approaches are being pursued to improve the processing result, including dynamic spatial oscillation of the laser beam. Gropp et al. (1995) and Geiger et al. (1996) used an axial beam oscillation in a low frequency range up to 100 Hz for reactive fusion cutting of 15 mm mild steel by a 2.2 kW CO_2-laser and introduced the notion “laser beam sawing” for this laser cutting variant. They applied a piezo-driven adaptive mirror, which resulted in a periodic change of the total focal length and the focus position of up to 10 mm. The authors reported an increase of the top kerf diameter and an improved rectangularity of the edges. Furthermore, they found a direct correlation between the applied oscillation frequency and the frequency of the striation pattern and a reduction of striation amplitude with frequency.

Mahrle and Beyer (2009) discussed an oscillation of the laser beam position tangential to the workpiece surface in cutting direction to control the cut front inclination. The approach aims to improve the energy transfer efficiency by adjusting the front inclination to the Brewster angle for increased absorption. Goppold et al. (2015 and 2017) investigated the potential of lateral beam oscillation experimentally. They examined different oscillation shapes, frequency and amplitude ranges for their influence on the process characteristics and achieved a productivity increase of up to 100 % and with comparable or enhanced cut quality. Recently, Pinder and Goppold (2021) investigated the physical fundamentals of beam oscillation based on thermographic analysis. They reported the modulation of kerf and front shape and the influence on energy deposition and temperature distribution in the processing zone.

2. Laser beam sawing, theory and experimental equipment

For the cutting trails of the performed laser sawing study a 4 kW multimode fiber laser YLR 4000 from IPG and a cutting head HP-SSL from Precitec were used. The optical configuration involved a fiber diameter of 50 µm, a collimation length of 100 mm and a focusing length of 125 mm. The resulting focus beam diameter is about 125 µm and the Rayleigh length is 1.26 mm. For the high frequency oscillation of the laser beam in axial direction two mirrors with variable curvature radius were integrated in the optical beam path (Fig 1 (a)). With this experimental equipment, sinusoidal oscillations of the focus position can be realized in a frequency range up to 4800 Hz. The maximal achievable focus offset is 12 mm, which corresponds to an oscillation amplitude A of 6 mm. In Fig 1 (b) the time-averaged beam profile for an oscillation amplitude of 5 mm is shown. Due to the oscillation, an almost constant beam radius is achieved over the entire focus offset range of 10 mm.

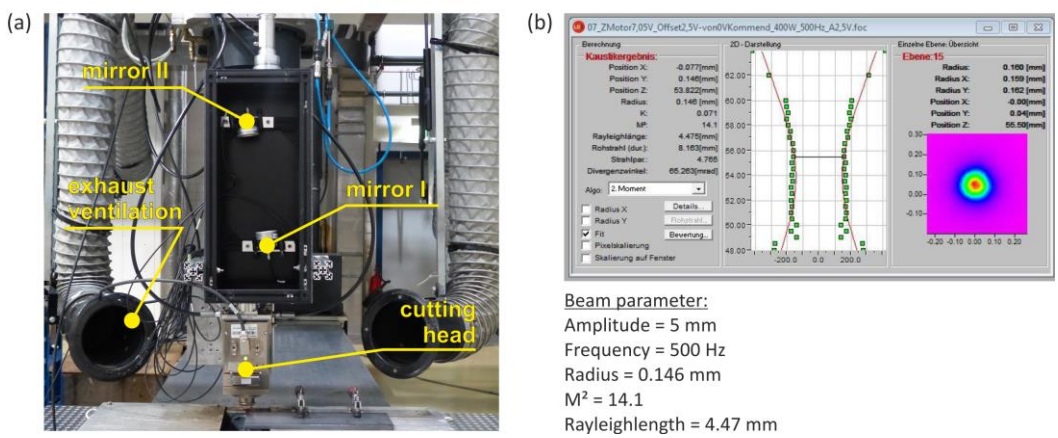

Fig. 1. (a) experimental setup for cutting trials with static and dynamic laser beam; (b) measured time averaged beam shape for an amplitude of 5 mm and an oscillation frequency of 500 Hz.

Contrary to dynamic beam shaping in x-y-direction, the oscillation of the focus position in axial direction allows for periodic changes of the local beam diameter at the top and the corresponding intensity distribution. In Fig 2 (a) the focus layer position over an oscillation period for different amplitudes and in 2 (b) the time-dependent beam diameter at the top of the material are shown for the applied optical configuration and a zero focus position of 2 mm underneath the top of the material. Relative to the appointed amplitude different behaviors of beam diameter and hence intensity distribution are observable. In case of small amplitudes the beam diameter at the top also shows an almost sinusoidal behavior with an average beam diameter almost equal to the focus diameter. For larger amplitudes only for the focus movement into the material, the beam diameter behaves sinusoidal. For the upward movement the beam diameter reaches its minimum size for the focus position at the top of the material and increases for the further upward movement. This results in an increasing average beam diameter at the top of the material and presumably in an increasing kerf width. In case of low oscillation frequency, the alternating beam diameter results in a variation of local kerf width. At high frequencies, the process will experience the oscillating beam as quasi-static with an average intensity distribution. The associated threshold value for the change of process reply is expected to give information about inherent processing frequencies for standard laser fusion cutting.

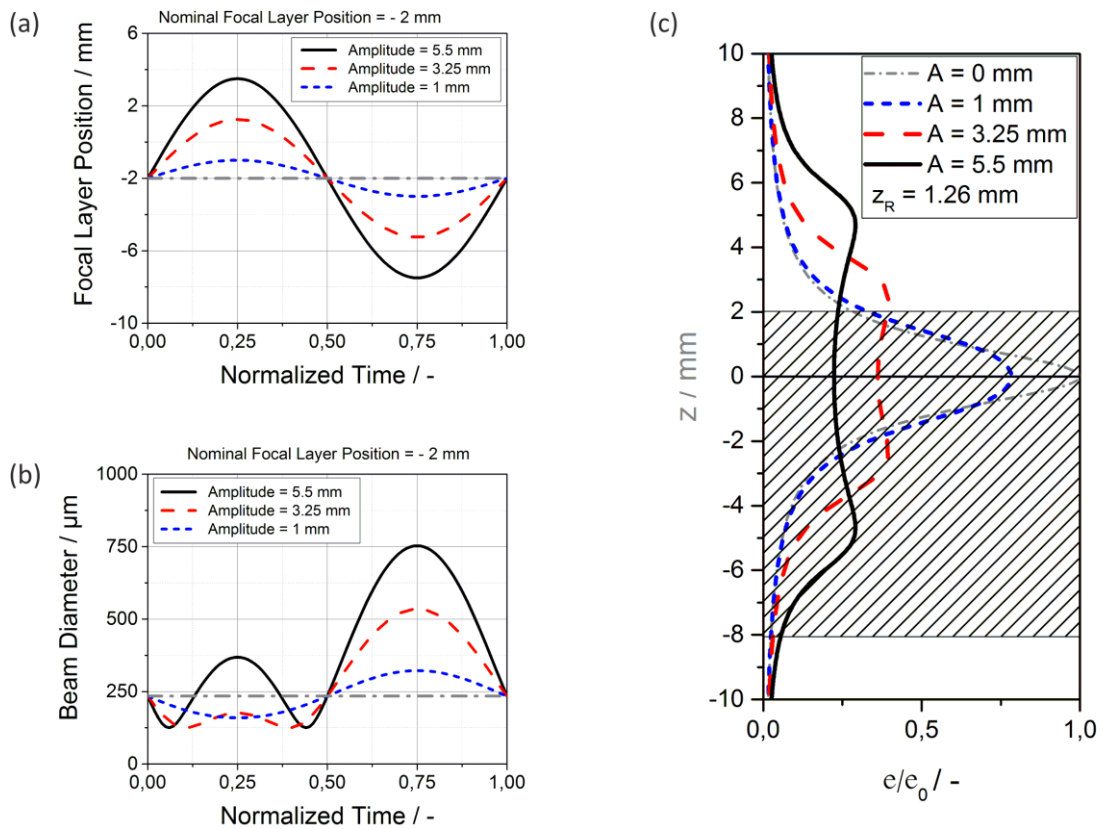

Fig. 2. (a) Focus layer position relative to top of material normalized over an oscillation period; (b) Beam diameter at the top of material normalized over an oscillation period; (c) Averaged energy distribution at the laser beam axis dependent on oscillation amplitude relative to material thickness of 10 mm (shaded area).

The time averaged energy distribution along the beam axis as limiting value for high frequencies is shown in Fig 2 (c). For a small oscillation amplitude of 1 mm the energy distribution is almost equal to the stationary laser beam profile, only with a leveled peak energy around the zero focus position. For higher amplitudes the range of high energy is broadened with an almost uniform level within the oscillation. Due to the sinusoidal oscillation movement, local maxima are formed near the reversal points. Due to these theoretical findings a smoothed energy distribution and hence more regular absorption of the laser power over the material thickness can be expected. It can be assumed that hot spots near the focal layer and the disposition to vaporization are reduced and the process stability is enhanced.

Nevertheless, the present study focusses on the influence of the axial oscillation and the modified energy distribution on the processing results in terms of kerf geometry and inherent process frequencies.

3. Experimental results

To determine the threshold frequency between direct structuring of the cut edge at very low oscillation frequencies to a more uniform impact of the time averaged intensity distribution cutting trials in the frequency range between 40 and 200 Hz were performed. The zero focus position was set to 2 mm underneath the top surface and a constant cutting velocity of 1.2 m/min was used. The oscillation amplitude was varied between 1 mm to 5.5 mm with an overall focus shift between 2 mm and 11 mm. For frequencies below 40 Hz no cuts were achieved for large amplitudes.

In Fig 3 determined threshold frequencies and characteristic cut edge structures are shown. Furthermore, only a slight dependency on the used amplitude was noted. Instructively, the threshold frequencies for direct patterning differ for particular cut edge areas. In case of an oscillation frequency between 40 Hz and 60-80 Hz a direct patterning of the cut edge over the entire oscillation range was detected.

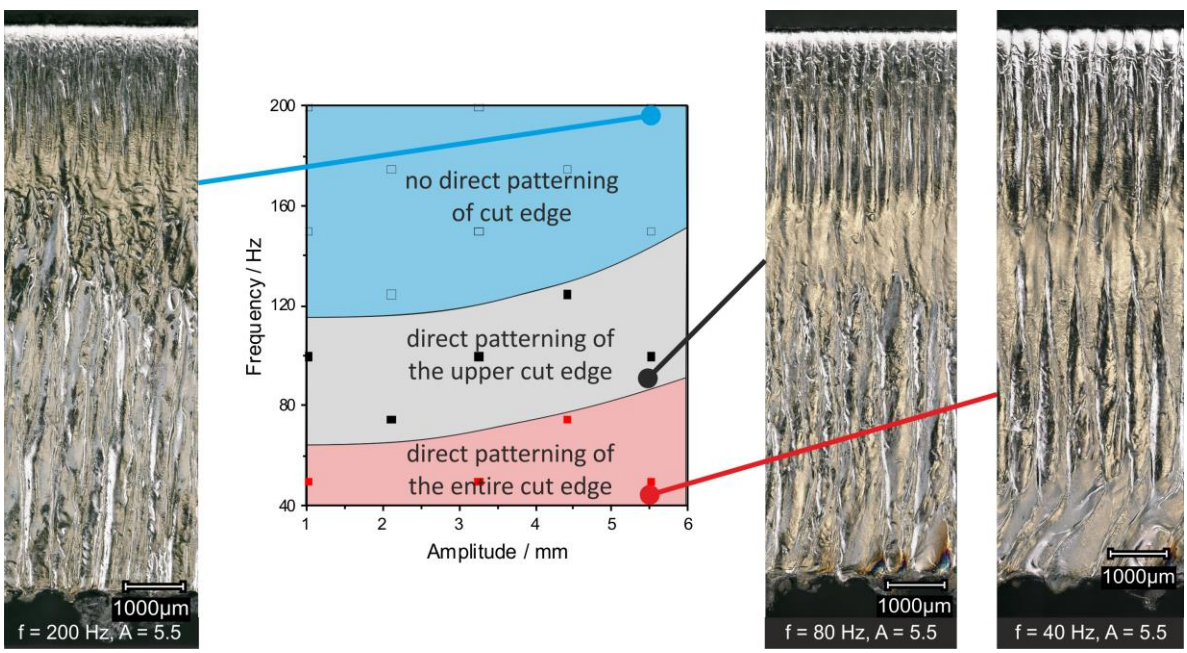

Fig. 3. Threshold frequencies for direct patterning of cut edges in 10 mm stainless steel by axial oscillation and characteristic cut edge appearance for an oscillation amplitude of 5.5 mm.

The wavelength of the resultant pattern corresponds to the ratio of the applied velocity to frequency. In case of 40 Hz and a cutting velocity of 1.2 m/min the lateral wavelength is about 500 µm. For frequencies between 80 Hz and 140 Hz the direct pattern is limited to the upper part of the kerf, at most to a depth of 4 mm, and the wavelength also correlates to the frequency. The bottom part is characterized by irregular striations without a clear frequency and the transition zone is very smooth. With increasing frequency the extension of the direct pattern is reduced and finally limited to a narrow band at the upper kerf corner. For frequencies higher than 160 Hz the direct pattern vanishes. However, the resulting structure differs from the static case. The top part of the cut edge is very smooth with fine and less marked striations. In the middle part only few striations are noted. The bottom half is characterized by an almost continuous layer of resolidified melt and slightly inclined but straight striations.

Another part of the study is the influence of oscillation amplitude on kerf geometry and cut edge structure. Using a frequency within the direct patterning range the area of influence of the oscillation amplitude can be determined. Fig 4 shows cut edges and kerf top views for a frequency of 100 Hz in dependence of the applied amplitude. The reference case without oscillation is characterized by a typical striation pattern for cutting of 10 mm stainless steel (Borkmann et al., 2019). For the application of axial oscillation the effective range becomes clear from the direct patterning area and shows a good correlation to the applied amplitude. For an amplitude of 1 mm the impact of oscillation is restricted to the effective range within the reversal points. From an amplitude of 3.5 mm on the oscillation influences the entire cut edge structure and for 6 mm amplitude the cut edge fundamentally differs from the reference case in terms of striation appearance and melt distribution.

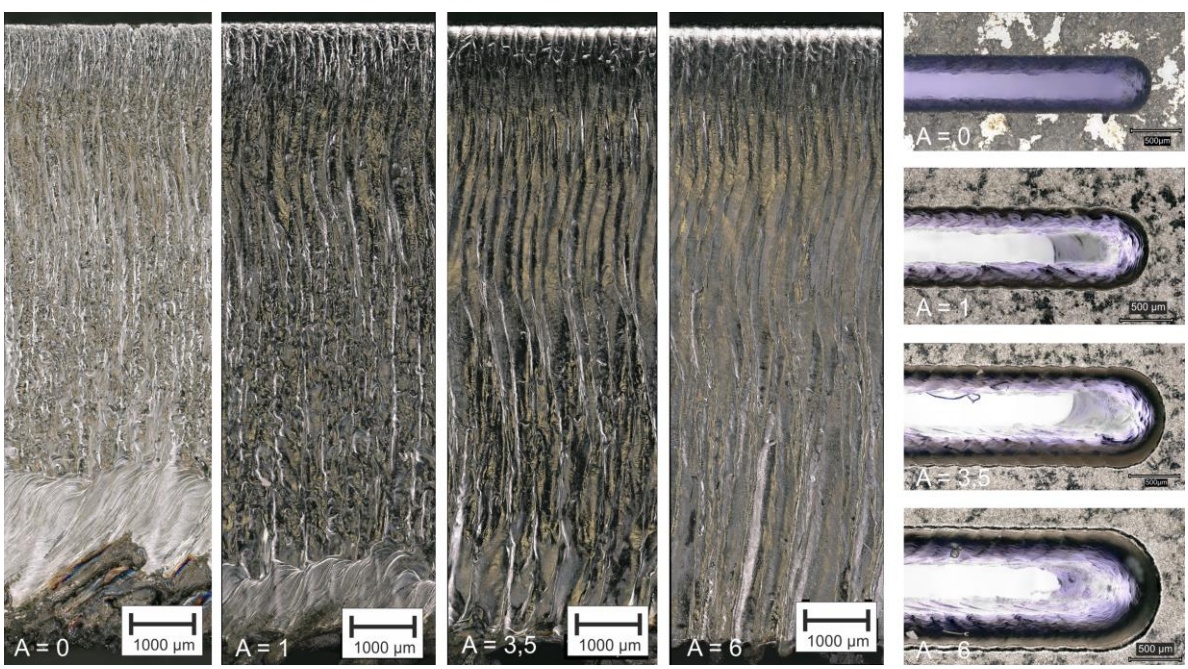

Fig. 4. Cut edge surface in dependence of oscillation amplitude for a frequency of 100 Hz and top views of the kerf near the front, focus position 2 mm below the top surface and constant velocity of 1.2 m/min.

For the reference case an extended area of resolidified melt at the lower part of the kerf is formed. It is assumed that a diverging part of the kerf geometry in the bottom region results in the separation of gas flow and in the insufficient melt removal with subsequent solidification due to the focus position of 3 mm below the top surface and the small Rayleigh length of 1.26 mm. For the sawing process, the reduction of the resolidification area can be detected with increased amplitude. For an amplitude of 1 mm there is still a small band of melt remains at the bottom edge whereas for 3.5 mm and 6 mm the melt adhesion inside the kerf is prevented. The analysis of the resulting kerf geometries reveals a widening of the kerf at the top and a reduction of kerf width at the bottom with increasing amplitude. For the reference case and an amplitude of 1 mm the kerf ratio (top diameter to bottom diameter near front location) is around 1. For an amplitude of 3.5 mm a ratio of 1.4 and for 6 mm a ratio of more than 2 is produced. In standard laser cutting with static beams, kerf ratios of this size are usually associated with a fundamental process bifurcation, massive melt accumulations within the kerf and quality reduction (Borkmann et al.; 2019). In contrast, for the sawing process with axial oscillation this failure is avoided and high quality cuts are achievable. Based on the kerf top views in Fig 4 it becomes apparent, that particularly the upper kerf is reshaped by the z-oscillation. In Fig 5 (a) the extracted kerf geometries for the reference case and for 6 mm amplitude are shown. The reference case is characterized by a pronounced bottleneck-shape with the waist around the focal layer position. The kerf shape is convergent above and divergent below this waist. With axial oscillation, the top kerf width is widened, the upper edge is smoothed and rounded and the bottleneck is significantly weakened and shifted downwards. The resulting kerf geometry for 6 mm amplitude is slightly convergent over the entire material thickness and the smallest diameter is located near the bottom corner. Also front shape, inclination and location relative to beam axis are modified, whereas the extension of the front in cutting direction is almost unaffected (Fig 5 (a)). The axial oscillation results in an enlarged region of moderate inclination at the upper front and the part of high inclination is shifted towards the bottom. Furthermore, the backward bending of the front, which is an indication for a process close to the achievable maximum of cutting speed, is not present for the oscillation with an amplitude of 6 mm. Additionally the front is shifted in cutting direction relative to beam and nozzle axis and the intersection of front and beam axis is shifted downwards.

The determined kerf geometry modifications due to axial oscillation result in fundamentally changed spatial boundary conditions for the cutting gas flow. To investigate the impact of the altered geometry on the gas flow additional CFD analyzes were performed.

4. Simulation of gas flow

For the CFD analysis, the commercial software package Ansys FLUENT is used. The study focusses on the influence of the kerf geometry on the global gas flow characteristics. The local gas boundary layer development is not subject of the present study, although it can be assumed that it has a significant influence on the overall result of the cutting process (Borkmann et al., 2021).

Kerf and front geometry were extracted from the corresponding experimental results and smoothed for simulation purposes (Fig 5 (a)). Additionally to the cut kerf volume, the simulation domain includes the bottom part of the nozzle, the gap between nozzle and top surface of the material and a run-out area underneath the kerf (Fig 5 (b)). Further, a symmetry plane aligned to cutting direction was applied due to a high degree of similarity of both cut edge shapes. The physical model is based on the Reynolds-averaged Navier-Stokes equations and solves the conservation equations of momentum, mass and energy under steady-state conditions with the use of the viscous SST k-ω turbulence model and standard wall functions. The cutting gas nitrogen was modelled according to the ideal gas law. The pressure at the gas inlet within the nozzle was specified as used in the corresponding experiments (1.8 MPa gas pressure, 3 mm conical nozzle and a distance of 0.5 mm). Ambient conditions were applied at the outlet.

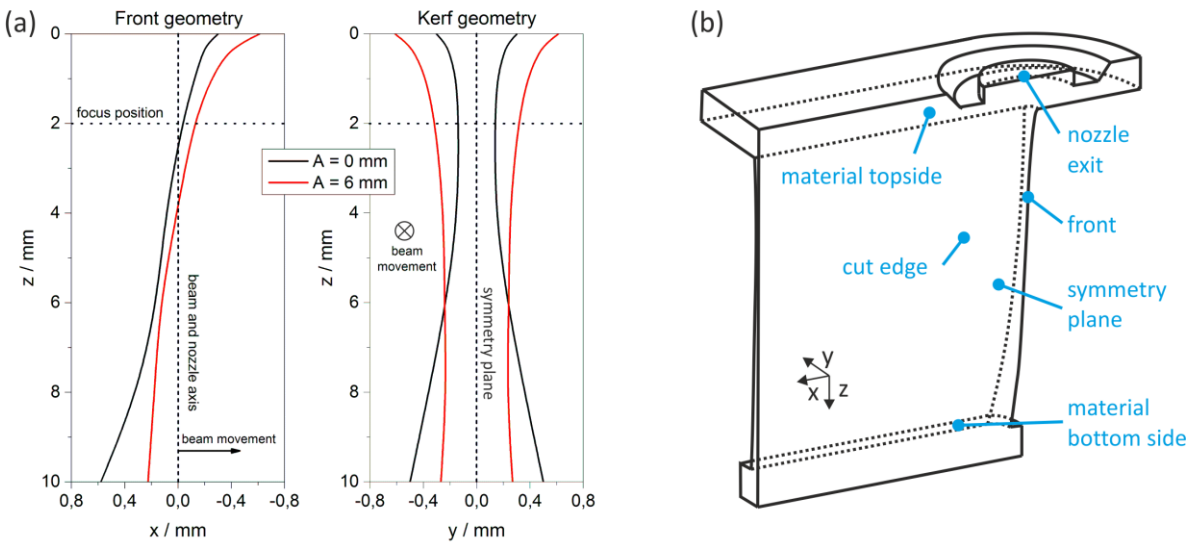

Fig. 5. (a) Front and kerf geometry for reference case at A = 0 mm and for A = 6 mm, smoothed for simulation purpose; (b) simulation domain for calculation of gas flow in laser cutting

The results of the CFD-analysis for the reference case and for an amplitude of 6 mm are shown in Fig 6. In Fig 6 (a) and (b) the velocity distribution at the symmetry plane and on a kerf cross section normal to the symmetry plane are depicted. In Fig 6 (c) and (d) the experimental cut edge and calculated wall shear lines (numerical equivalent to oil flow visualization) at the modeled cut edge are shown. The gas flows of both cases differ in fundamental aspects. Without oscillation the pronounced bottleneck shape determines the resulting gas flow. Within the convergent part above the smallest diameter the gas flow is redirected to the back, especially underneath the edge of the nozzle. For that part of the flow the expansion and acceleration of the high pressure cutting gas is directed backwards. The gas flow close to the front is hardly accelerated and reaches at first the speed of sound around the kerf waist. Downstream, the gas flow strongly expands and accelerates due to the distinct divergent kerf shape. The gas pressure decreases and finally falls below ambient pressure. Through adapting to the ambient conditions by shocks, the gas flow globally separates from the cut edge and an open recirculation region is formed between cut edge and core gas flow. The open recirculation sucks in ambient atmosphere and results in undesirable oxidation of the cut edge as seen in Fig 6 (c). The global separation of the cutting gas flow is associated with a dramatic decrease and even reversal of shear forces transferred to the melt and leads to the failure of melt removal. The extent of the gas detachment corresponds very well to the experimentally determined melt accumulations at the cut edge.

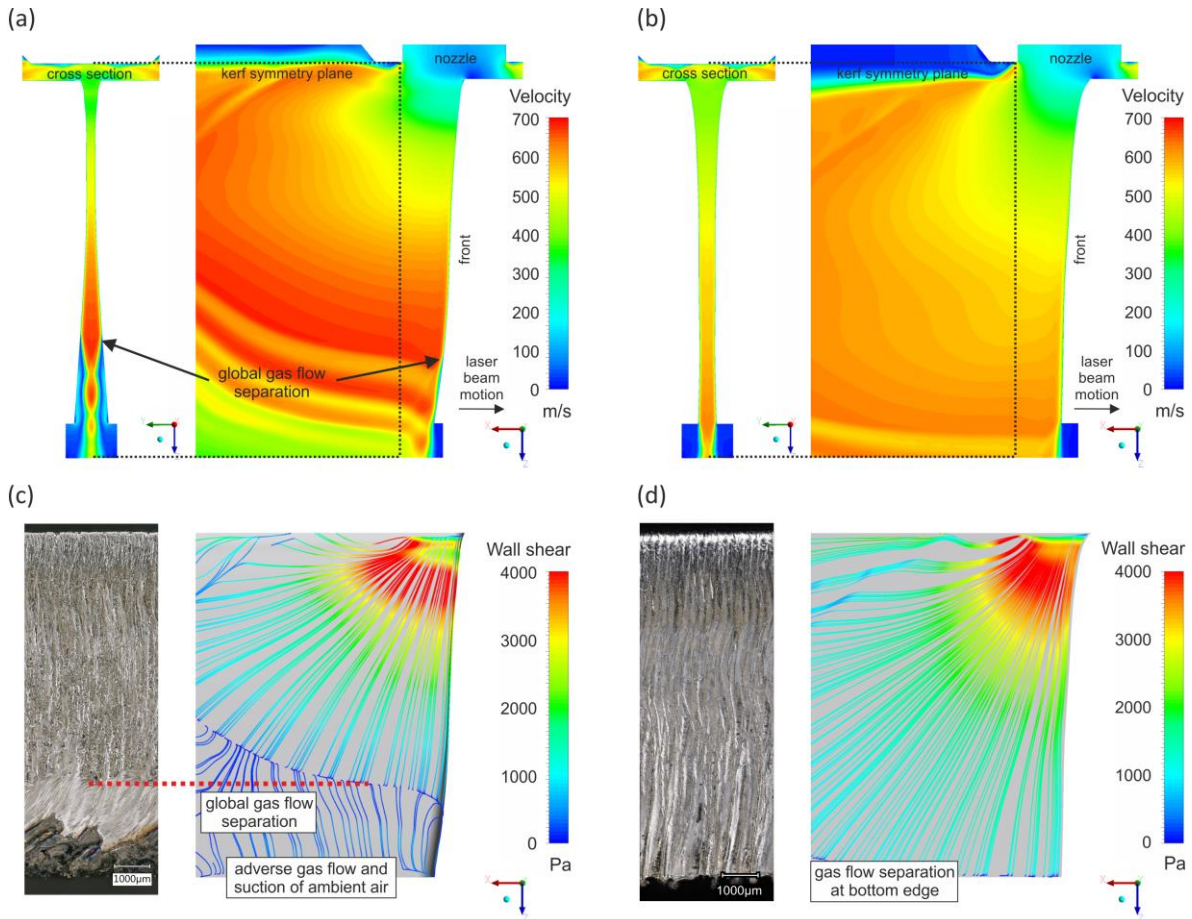

Fig. 6. (a) Velocity distribution at symmetry and at marked cross section for reference case with A = 0; (b) Velocity distribution at symmetry and at marked cross section for A = 6 mm at f = 100 Hz; (c) cut edge and calculated wall shear lines at front and edge colored by local wall shear for reference case with A = 0; (d) cut edge and calculated wall shear lines colored by local wall shear for A = 6 mm at f = 100 Hz.

In case of the axial oscillation with 6 mm amplitude the slightly convergent kerf shape determines the gas flow. Underneath the nozzle edge the backward redirection of the gas flow is significantly reduced and extended along the entire kerf. The gas flow close to the front reaches sonic speed within the uppermost part of the kerf and is then slowly and steadily accelerated along the entire kerf. Inside the cut kerf the gas pressure remains above the ambient pressure and only at the lower edge the sudden adjustment to ambient condition takes place. Consequently, the gas flow is attached to the complete front and cut edge near the processing zone. As a result, high values for the shear stress (Fig 6 (d)) are predicted which ensure the required melt removal.

The CFD analysis enables the evaluation of gas mass flow rates and the determination of the utilized gas amount inside the kerf. If the nozzle spacing is small relative to its diameter, the kerf acts as an extension of the nozzle and the kerf shape determines the resulting mass flow through the system. Additionally, the portion of the mass flow coupled into the cut kerf is mainly determined by the area of intersection between the nozzle

and the kerf. Because of that, the actual kerf geometry influences the total mass flow and the proportion of utilized gas amount. For the reference case, a total mass flow of 19.4 g/s was calculated of which 17.9 % were coupled into the kerf. For the process with axial oscillation, the total mass flow increased to 22.6 g/s of which 38.0 % were utilized. Therefore, the overall gas flow with axial oscillation through the slightly convergent and widened kerf is 2.5 times as high as for the reference case.

5. Summary and Conclusions

Under the conditions of the performed laser beam sawing study, a frequency of 60 - 80 Hz was determined as the threshold value to direct structuring at the lower edge. The value of the equivalent wavelength with respect to the cutting velocity follows to 333 – 240 µm for one oscillation period. The calculated wavelength is quite similar in magnitude to the striation wavelength for the reference case at the lower cut edge. A similar conclusion applies to the threshold frequency at the upper cut edge. Here a threshold frequency of 160 Hz is identified in this study, which corresponds to an equivalent wavelength of 125 µm. For frequencies above the threshold the cut edge is characterized by a more random striation pattern, though it is different to the reference case of conventional cutting. Especially a changed distribution of melt remains and bending of striations could be observed.

The major effects of axial oscillation are closely related to its kerf shaping capability. Due to the enlargement of the virtual Rayleigh length and the more homogeneous energy distribution over the complete material thickness, a bottleneck shape of the kerf with pronounced convergent and divergent parts is avoided. The axial oscillation resulted in a widened, slightly convergent and even kerf shape. Consequent advantages for the gas flow dynamics could be revealed by CFD simulations with consideration of realistic kerf shapes and actual boundary conditions. The study emphasizes the decisive influence of the kerf shape on the resulting gas flow characteristics and the momentum transfer to the molten material. It was shown that in case of axial oscillation an advantageous gas flow was achieved over the entire processing area and the gas flow rate through the kerf was 2.5 times as high as for the reference case. Possibly, these advantages can be transferred to a gas pressure reduction with consistent cut quality. Additionally, the kerf ratios (top width to bottom width) generated with axial oscillation indicate a decreased susceptibility to process failures normally occurring for low focal layer positions in conventional laser fusion cutting. Furthermore, the absent backward bending of the front near the bottom and the shifted intersection of front and beam axis suggest a better utilization of laser power and possibly higher achievable cutting speeds.

Particularly, the authors point out the use of axial beam oscillation in combination to dynamic beam shaping approaches in x and y direction (Wetzig et al., 2020). With such a technology, it should be possible to address a multitude of control parameters to expand the application area of laser beam cutting to higher material thicknesses due to the increased virtual Rayleigh length, the balanced energy distribution over the material and the improved gas utilization.

Acknowledgements

The study was partly financed by the German Research Foundation (DFG) within the project “Evaluierung dynamischer Lösungsansätze zur Optimierung des Inertgasschneidens von Dickblech mit Laserstrahlquellen hoher Strahlqualität”, Contract No BE 1875/36-1. The authors highly appreciate the financial support.

References

Borkmann, M., Mahrle, A., Beyer, E.,Leyens, C., 2021. Laser fusion cutting: evaluation of gas boundary layer flow state, momentum and heat transfer, Materials Research Express, 8(2021) 036513. doi: 10.1088/2053-1591/abed12.

Borkmann, M., Mahrle, A., Beyer, E.,Leyens, C., 2019. Cut Edge Structures and Gas Boundary Layer Characteristics in Laser Beam Fusion Cutting, Lasers in Manufacturing conference 2019. Munich, Germany.

Geiger, M., Schuberth, S., Hutfless, J., 1996. CO_2 laser beam sawing of thick sheet metal with adaptive optics, Welding in the World 37, p. 5 – 11.

Goppold, C., Pinder, T., Herwig, P., Mahrle, A., Wetzig, A., Beyer, E., 2015. Beam oscillation – Periodic modification of the geometrical beam properties, Lasers in Manufacturing conference 2015. Munich, Germany.

Goppold, C., Pinder, T., Herwig, P., 2017. Dynamic beam shaping for thick sheet metal cutting, Lasers in Manufacturing conference 2017. Munich, Germany.

Gropp, A., Hutfless, J., Schuberth, S., Geiger, M., 1995. Laser beam cutting, Optical and Quantum Electronics 27, p. 1257-1271. doi: 10.1007/BF00326480.

Mahrle, A., Beyer, E., 2009. Theoretical aspects of fibre laser cutting, Journal of Physics D: Applied Physics 42, p. 1-9, doi: 10.1088/0022-3727/42/17/175507.

Pinder, T., Goppold, C., 2021. Understanding the Changed Mechanisms of Laser Beam Fusion Cutting by Applying Beam Oscillation, Based on Thermographic Analysis, Applied Sciences 11, p. 921, doi: 10.3390/app11030921.

Steen, W. M., 1998. Laser Material Processing. Springer Verlag London Limited, London.

Wetzig, A., Herwig, P., Borkmann, M., Goppold, C., Mahrle, A., Leyens, C., 2020. Fast beam oscillations improve laser cutting of thick materials, PhotonicsViews 3/2020, 26-31.